INVERSE KINEMATICS AND SINGULARITY ANALYSIS OF A KINEMATICALLY REDUNDANT PARALLEL ROBOT

Thanh-Trung Do[1,*], Van-Truong Nguyen[1]

DOI: http://doi.org/10.57001/huih5804.2025.267

ABSTRACT

This work presents the inverse kinematics and singularity conditions of a kinematically redundant planar parallel robot (3-RRRR) with six degrees of freedom. Due to the existence of infinitely many solutions in the inverse kinematics problem and singular configurations within the workspace, an analytical method based on singularity conditions is proposed to address these challenges. As a result, the inverse kinematic solutions are derived in an analytical form, enabling real-time control. Furthermore, the approach allows the robot to avoid singular configurations and expand its usable workspace. Numerical simulations are conducted to demonstrate the effectiveness of the proposed method.

Keywords: *Redundant parallel robot, singularity analysis, inverse kinematics.*

[1]School of Mechanical and Automotive Engineering, Hanoi University of Industry, Vietnam

[*]Email: trungdo@haui.edu.vn

Received: 01/3/2025

Revised: 25/4/2025

Accepted: 25/7/2025

1. INTRODUCTION

The field of robotics has seen significant advancements over the past few decades. Parallel robots, in which the moving platform are connected to the base using multiple kinematic chains (legs), are prominent candidates due to their inherent advantages in terms of rigidity, precision, and heavy loads [1]. However, parallel robots have some disadvantage such as workspace limitation and specially, singularity within the workplace. In addition, the kinematic and dynamic problems of parallel robots are quite complicated, especially for real-time applications.

Generally, there are three types of parallel robots [2, 3, 9, 10]: (1) non-redundant parallel robots, (2) parallel robots with actuation redundancy, and (3) parallel robots with kinematic redundancy. Compared to the first type, the second type offers advantages such as eliminating singularities, increasing stiffness, and improving acceleration capabilities because more actuators or even new legs are integrated into the robot structure. However, since the number of actuators exceeds the number of degrees of freedom (DOF) of the robot, controlling this type becomes challenging, particularly in generating internal forces and moments, as well as distributing the forces and moments among the actuators. For the third type, redundant links and actuators are incorporated into the non-redundant robot structure to expand the workspace, avoid singularities, and prevent collisions between the legs [4, 5]. Since the number of actuators equals the robot's DOFs, the third type does not introduce antagonistic forces, which are unavoidable in the second type. In order to control of the kinematically redundant parallel robots for singularity avoidance, singularity conditions need to be formulated efficiency.

Inverse kinematics and singularity avoidance plays a pivotal role in controlling parallel robots. In kinematically redundant systems, multiple solutions for a given task may exist. This problem requires sophisticated algorithms to find solutions that optimize robot performance while avoiding singularity configurations. At these configurations within the workspace, the robot gains/loses degrees of freedom or its workspace, leading to unstable behavior.

This paper aims to investigate the inverse kinematics and singularity analysis of the planar kinematically redundant 3-RRRR parallel robot proposed in [5]. Here, the notations R and R stand for active and passive revolute joints, respectively. We focus on modeling and solving the inverse kinematics problem and formulate singularity conditions in order to obtain kinematic solutions in analytical form.

The remainder of this paper is organized as follows: Section 2 introduces the kinematic model of the 3-RRRR parallel robot, including the constraint equations derived using the subsystem technique. Subsequently, the inverse kinematic solutions are obtained using the predetermined redundant coordinates. From constraint equations, the singularity conditions are formulated in analytical forms in Section 3. Next, Section 4 discusses numerical simulations for singularity avoidance and the inverse kinematic problem. Finally, the conclusions of the study are provided in Section 5.

2. KINEMATIC MODELING

The planar kinematically redundant 3-RRRR parallel robot shown in Fig (1a) was firstly introduced by Wen and Gosselin in [5]. This robot is derived from the non-redundant 3-RRR parallel robot (see [6]) by adding redundant links B_iP_i to the non-redundant legs $O_iA_iB_i$, for $i = (1, 2, 3)$. With the use of redundant links, one can enlarge the workspace and avoid the second kind of singularity (direct singularity) in the non-redundant parallel robot.

The 3-RRRR robot has six degrees of freedom, consisting of three identical legs connected to the moving platform $P_1P_2P_3$. Each leg is driven by two motors, in which a driven revolute joint is denoted by R and marked in orange in Fig. (1a). For kinematic modeling, the subsystem technique is used to convert the robot system with the complex mechanism into simpler mechanisms. Thus, the robot is considered as four subsystems: one subsystem is combined by the moving platform with redundant legs (see Fig. (1b)) and other subsystems are three legs, e.g., the third leg is shown in Fig. (1c).

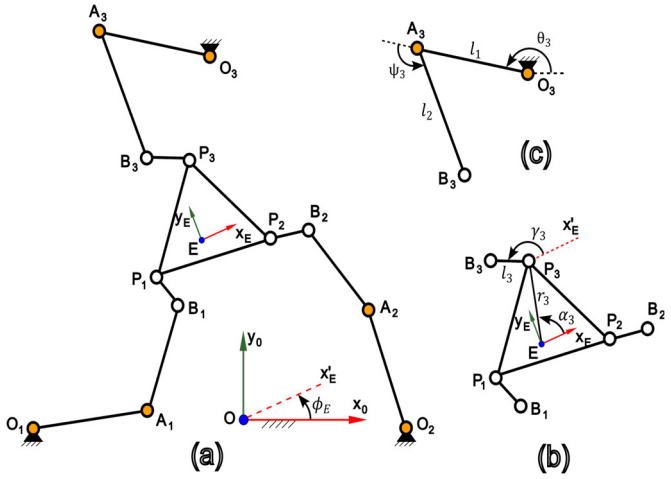

Fig. 1. Kinematic modeling and geometric parameters of the 3-RRRR robot with 6 DOFs: (a) is the complete model; (b) is the moving platform with redundant links; (c) is the model of one leg

We use two coordinate frames for modeling: the base frame (the inertial frame) Ox_0y_0, and the moving frame Ex_Ey_E attached to the moving platforms at E. Position of the moving platform with respect to O in Ox_0y_0 is defined by a position vector $\mathbf{p}_E = [x_{E,}\, y_{E,}]^T$. The orientation of the moving platform with respect to Ox_0y_0 is determined by an angle ϕ_E. The relative motion of a redundant link B_iP_i with respect to the moving frame Ex_Ey_E is defined by an angle γ_i. Two active joint coordinates, denoted by (θ_i, ψ_i), are used to describe the leg's motion.

2.1. Constraint equations

Because the leg $O_iA_iB_i$ is connected to the moving platform using the redundant link B_iP_i at the revolute joint B_i, constraint positions are established as follows:

$$\mathbf{f}_i = \begin{bmatrix} x_{O_i} + l_1\cos(\theta_i) + l_2\cos(\theta_i + \psi_i) - x_{B_i} \\ y_{O_i} + l_1\sin(\theta_i) + l_2\sin(\theta_i + \psi_i) - y_{B_i} \end{bmatrix} = \mathbf{0} \quad (1)$$

with

$$\begin{aligned} x_{B_i} &= x_E + r_i\cos(\phi_E + \alpha_i) + l_3\cos(\phi_E + \gamma_i) \\ y_{B_i} &= y_E + r_i\sin(\phi_E + \alpha_i) + l_3\sin(\phi_E + \gamma_i) \end{aligned} \quad (2)$$

and $l_1, l_2, l_3, r_i, \alpha_i$ denotes geometric parameters of the robot, and (x_{O_i}, y_{O_i}) are position of O_i in Ox_0y_0. For $i = 1, 2, 3$, constraint equations of the robot can be written in a compact form as:

$$\mathbf{f}(\mathbf{q}) = \left[\mathbf{f}_1^T, \mathbf{f}_2^T, \mathbf{f}_3^T\right]^T = \mathbf{0} \quad (3)$$

where $\mathbf{q}$ is the vector of generalized coordinates:

$$\mathbf{q} = [\theta_1, \psi_1, \theta_2, \psi_2, \theta_3, \psi_3, \gamma_1, \gamma_2, \gamma_3, x_E, y_E, \phi_E]^T$$

The nonlinear system (3), containing six independent equations and twelve generalized coordinates, describes position relationships among all subsystems. From the Eq. (3), the corresponding velocity and acceleration relationships can be derived easily. It is important to note that constraint equations of the robot can be formulated in different ways depending on how the subsystems are considered, as well as how the generalized coordinates are defined.

2.2. Inverse kinematics

To solve the inverse kinematic problem of the 3-RRRR robot, we assume that the position and orientation $(x_{E,}\, y_{E,}\, \phi_E)$ of the moving platform are given. From six constraint equations above, we need to find nine unknowns: $\mathbf{q}_u = [\theta_1, \psi_1, \theta_2, \psi_2, \theta_3, \psi_3, \gamma_1, \gamma_2, \gamma_3]^T$. Since the number of equations is fewer than the number of unknowns, the system possesses infinitely many solutions.

In this study, the angles γ_i for $i = (1, 2, 3)$ will be predetermined to avoid direct singularities within the

robot's workspace (see the next section for details). Consequently, we have six equations with six unknowns. Therefore, the inverse kinematic problem of this robot is similar to the 2-RR serial robot presented in robotic textbooks. Its kinematic solutions can be found from Eq. (1) as follows:

$$\cos(\psi_i) = \frac{x_{B_i}^2 + y_{B_i}^2 - l_1^2 - l_2^2}{2l_1 l_2}$$
$$\Rightarrow \psi_i = \pm\arccos\left(\frac{x_{B_i}^2 + y_{B_i}^2 - l_1^2 - l_2^2}{2l_1 l_2}\right) \quad (4)$$

where x_{B_i}, y_{B_i} are computed using Eq. (2). After obtaining ψ_i, one can compute θ_i as:

$$\theta_i = \arctan\left(\frac{(l_1 + l_2\cos(\psi_i))y_{B_i} - l_2\sin(\psi_i)x_{B_i}}{(l_1 + l_2\cos(\psi_i))x_{B_i} + l_2\sin(\psi_i)y_{B_i}}\right) \quad (5)$$

For the given values $(x_E, y_E, \phi_E, \gamma_1, \gamma_2, \gamma_3)$, we obtain two branch solutions from Eq. (4). Therefore, the inverse kinematic problem of the robot has a total of 8 different solutions.

3. SINGULARITY ANALYSIS

For non-redundant parallel robots, three types of singularities were discussed in [7]. Basically, the singularity analysis problem of a parallel robot is formulated based on the relationship between the input and output speeds and the determinant of the Jacobian matrices. For the 3-RRRR robot, authors in [5] established $(3x3)$ and $(3x6)$ Jacobian matrices and using the Plücker lines to detect singular configurations. The singularity conditions derived using this approach are very complicated because it related to the determinant of the Jacobian matrices.

Based on the approach proposed in [8], we will establish singularity conditions of the 3-RRRR robot in analytical forms. To do this, the vector $\mathbf{q}$ is decomposed into two parts: the vector of active joint coordinates $\mathbf{q}_a = [\theta_1, \psi_1, \theta_2, \psi_2, \theta_3, \psi_3]^T$ and the vector of passive coordinates $\mathbf{q}_p = [x_E, y_E, \phi_E, \gamma_1, \gamma_2, \gamma_3]^T$. By differentiating Eq. (3) with respect to time, one leads to:

$$\mathbf{\Phi}_a \dot{\mathbf{q}}_a = \mathbf{\Phi}_p \dot{\mathbf{q}}_p \quad (6)$$

where $\mathbf{\Phi}_a, \mathbf{\Phi}_p$ are $(6x6)$ Jacobian matrices (not written here due to space limitations) depending on $\mathbf{q}_a, \mathbf{q}_p$ respectively, with:

$$\mathbf{\Phi}_a = \frac{\partial \mathbf{f}}{\partial \mathbf{q}_a}, \quad \mathbf{\Phi}_p = \frac{\partial \mathbf{f}}{\partial \mathbf{q}_p} \quad (7)$$

Inverse kinematic singularity: if the singularity condition, $\det(\mathbf{\Phi}_a) = 0$, is fulfilled the vector $\dot{\mathbf{q}}_a$ can be non-zero even $\dot{\mathbf{q}}_p = \mathbf{0}$. In this configuration, the motion of motors does not affect to the motion of the moving platform and redundant links, i.e., the robot loses of one or more degree(s) of freedom.

From Eq. (3) and Eq. (7), the expression $\det(\mathbf{\Phi}_a)$ is expressed as:

$$\det(\mathbf{\Phi}_a) = l_1^3 l_2^3 \sin(\psi_1)\sin(\psi_2)\sin(\psi_3) \quad (8)$$

This condition occurs when $\psi_i = k\pi$, where k is an integer number. Geometrically, one or more legs are fully stretched or folded.

Direct kinematic singularity: if the singularity condition, $\det(\mathbf{\Phi}_p) = 0$, is fulfilled. The vector $\dot{\mathbf{q}}_p$ can be non-zero even all active joints are locks ($\dot{\mathbf{q}}_a = \mathbf{0}$ and $\mathbf{\Phi}_p \dot{\mathbf{q}}_p = \mathbf{0}$). In this configuration, the passive coordinates can move locally, i.e., the robot gains of one or more degree(s) of freedom.

From Eq. (3) and Eq. (7) and after some manipulations, the expression $\det(\mathbf{\Phi}_p)$ is obtained using Maple software as follows:

$$\det(\mathbf{\Phi}_p) = l_3^3\big(r_1\sin(\alpha_1 - \gamma_1)\sin(\gamma_2 - \gamma_3) + r_2\sin(\alpha_2 - \gamma_2)\sin(\gamma_3 - \gamma_1) + r_3\sin(\alpha_3 - \gamma_3)\sin(\gamma_1 - \gamma_2)\big) \quad (9)$$

To the best of our knowledge, Eq. (9) is obtained for the first time in this work. It can be seen that $\det(\mathbf{\Phi}_p)$ scales with l_3^3 depending only on angles $(\gamma_1, \gamma_2, \gamma_3)$ and the geometrical parameters of the moving platform, while the angle ϕ_E has been completely eliminated. Based on this expression, the direct singularity problem of the 3-RRRR robot can be solved for any configuration. Numerical simulations will be conducted in the next section to illustrate the advantages of our approach.

4. SIMULATION RESULTS

Numerical simulations for the direct singular problem of the 3-RRRR robot are presented in this section. Therefore, angles $\gamma_1, \gamma_2, \gamma_3$ can be selected appropriately to avoid singular configurations. These angles are used to solve the inverse kinematic problem.

The geometrical parameters of the robot used for numerical simulations are: $l_1 = l_2 = 0.55\text{m}$, $l_3 = 0.05\text{m}$, $r_1 = r_2 = r_3 = r = 0.08\text{m}$; $\alpha_1 = \frac{7\pi}{6}, \alpha_2 = -\frac{\pi}{6}, \alpha_3 = \frac{\pi}{2}$ rad. In addition, position vectors of legs are given by: $x_{O_1} = 0.0, y_{O_1} = 0.0$, $x_{O_2} = 1.0, y_{O_2} = 0.0$ and $x_{O_3} = 0.5, y_{O_3} = 0.866\text{m}$. The angles γ_1, γ_2 and γ_3 are varied within the interval $[-180, 180]$ degree.

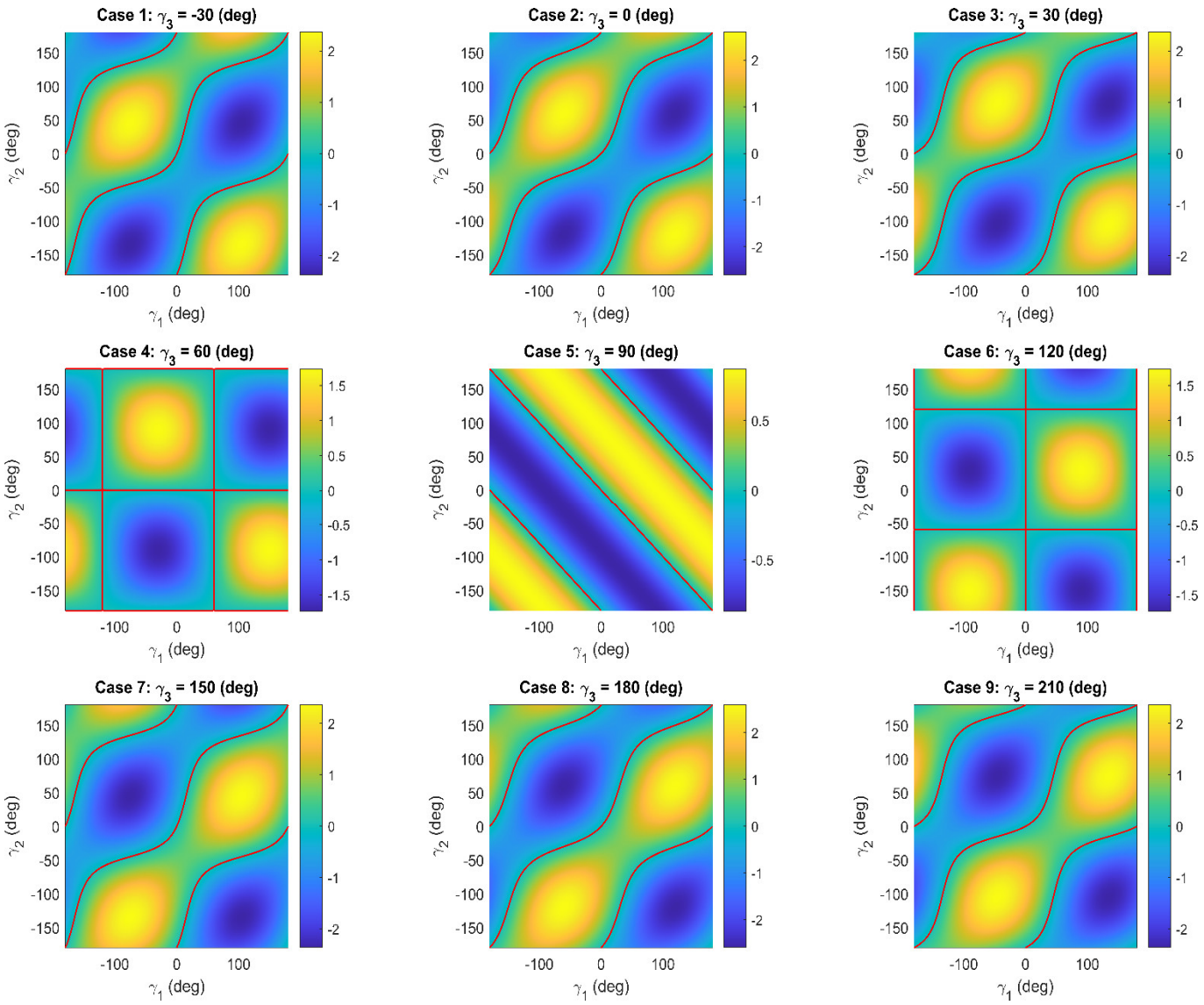

Fig. 2. Simulation of direct kinematic singularities of the 3-RRRR parallel robot

For each value $(\gamma_1, \gamma_2, \gamma_3)$, one can compute $\det(\mathbf{\Phi}_p)$ using Eq.(9). For example, γ_3 is held constant at different values and other angles γ_1, γ_2 are discretized with a discrete step of 1 degree. Nine singular maps (corresponding to 9 cases) are exemplarily shown in Fig. 2. The color bar on the right of each subfigure is used to describe values of $\det(\mathbf{\Phi}_p)$, where the blue color represents $\det(\mathbf{\Phi}_p) < 0$, and green-yellow color represent $\det(\mathbf{\Phi}_p) > 0$. The singular curves, $\det(\mathbf{\Phi}_p) = 0$, are plotted in red color. For the fourth, fifth and sixth cases, the singular curves become linearly. Note that the value of $\det(\mathbf{\Phi}_p)$ must always keep negative or positive to avoid direct singularities.

Depending on the motion of the moving platform in the robot workspace and based on the singularity maps shown in Fig. 2, three angles $\gamma_1, \gamma_2, \gamma_3$ can be chosen in many ways to avoid direct singularities. For example, the motion of the moving platform on a circle is given by: $x_E = 0.5 + 0.4\cos(\frac{2\pi}{T}t)$, $y_E = 0.2887 + 0.4\sin(\frac{2\pi}{T}t)$ m, $t \in [0, T]$, $T = 4$ s and $\phi_E = 0$, it is possible to select $\gamma_1 = -80$, $\gamma_2 = 45$, $\gamma_3 = 150$ deg (see case 7 in Fig. 2) to avoid singular configurations because $\det(\mathbf{\Phi}_p) = -2.357 rl^3$. Consequently, simulation results for inverse kinematics are plotted in Fig. 3.

It can be seen from Fig. 3 that the redundant coordinates are assumed to be hold constant during the motion in order to avoid direct singularities. This task can be done based on model-based controllers or intelligent controllers such as in [3, 11] to control the robot. This is the subject of our research in the future.

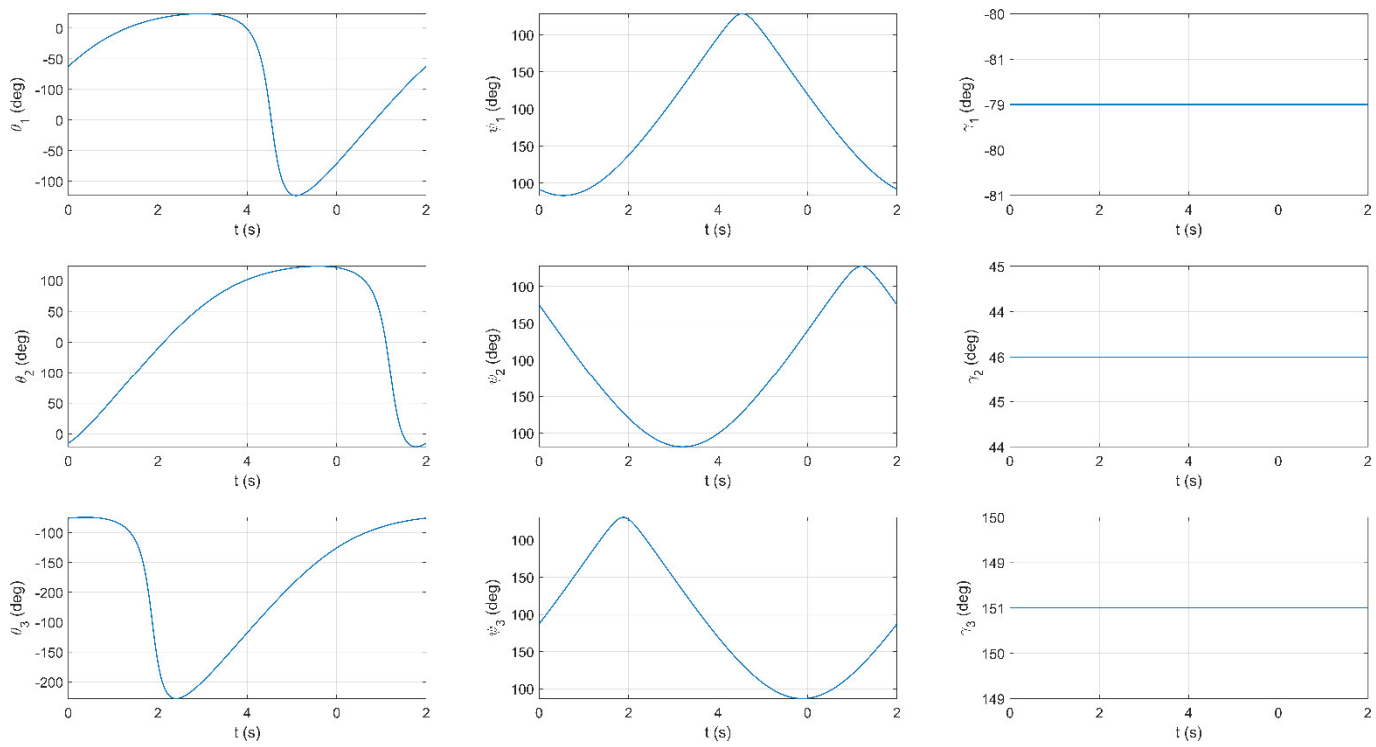

Fig. 3. Inverse kinematic solution of the 3-RRRR parallel robot with free-singularity avoidance

5. CONCLUSION

This paper has explored inverse kinematic solutions and singularity conditions for the kinematically redundant 3-RRRR parallel robot. Analytical formulations of these conditions were derived from the constraint equations. Numerical simulation results for direct kinematic singularity demonstrated that these conditions can effectively guide the selection of redundant coordinates for inverse kinematic solutions, helping to avoid singular configurations within the robot's workspace. The proposed formulation can be further extended to identify optimal redundant coordinates for path planning with singularity avoidance, as well as to develop advanced model-based or intelligent controllers for kinematically redundant planar parallel robots.

ACKNOWLEDGMENT

The work described in this paper was supported by Ha Noi University of Industry.

REFERENCES

[1]. Merlet J. P., *Parallel Robots* (2nd ed.). Springer, Berlin, 2006.

[2]. Gosselin C., Schreiber L.T, "Redundancy in parallel mechanisms: A review," *Applied Mechanics Reviews*, 70(1), 2018.

[3]. Cheng H., Yiu Y.K., Li Z., "Dynamics and control of redundantly actuated parallel manipulators," *IEEE/ASME Transactions on mechatronics*, 8(4), 483-491, 2003.

[4]. Ebrahimi I., Carretero J.A., Boudreau R., "3-PRRR redundant planar parallel manipulator: Inverse displacement, workspace and singularity analyses," *Mechanism and Machine Theory*, 42(8), 1007-1016, 2007.

[5]. Wen T., Gosselin C., "Kinematically redundant hybrid robots with simple singularity conditions and analytical inverse kinematic solutions," *IEEE Robotics and Automation Letters*, 4 (4), 3828-3835, 2019.

[6]. Gosselin C., Angeles J., "The optimum kinematic design of a planar three-degree-of-freedom parallel manipulator," *Journal of Mechanisms, Transmissions, and Automation in Design*, 110(1), 35-41, 1988.

[7]. Gosselin C., Angeles J., "Singularity analysis of closed-loop kinematic chains," *IEEE transactions on robotics and automation*, 6(3), 281-290, 1990.

[8]. Bandyopadhyay S., Ghosal A., "Analysis of configuration space singularities of closed-loop mechanisms and parallel manipulators," *Mechanism and Machine Theory*, 39(5), 519-544, 2004.

[9]. Müller A., "Internal preload control of redundantly actuated parallel manipulators-its application to backlash avoiding control," *IEEE transactions on robotics*, 21 (4), 668-677, 2005.

[10]. Kotlarski J., Do T.T., Heimann B., "Optimization strategies for additional actuators of kinematically redundant parallel kinematic machines," in *IEEE International Conference on Robotics and Automation*, 2010.

[11]. Nguyen V. T., Lin C. Y., Su S. F., Tran Q. V., "Adaptive chattering free neural network based sliding mode control for trajectory tracking of redundant parallel manipulators," *Asian Journal of Control*, 21(2), 908-923, 2019.